Development and testing of a new instrument for researching on cancer treatment technologies based on magnetic hyperthermia

Special Issue on Power Electronics in Biomedical Applications, 2015

Abstract— A power electronics circuit allows the generation of high frequency magnetic field that can be used to increase the temperature of cancer cells previously invaded with magnetic nanoparticles. The circuit designed for this purpose is a high frequency phase-shift inverter implemented with SiC devices and natural Zero Voltage Switching (ZVS). The inductive load has been optimized to increase as much as possible the magnetic field at the center taking into account the physical restrictions. Into this inductor, an adiabatic probe filled with nanoparticles is placed being the main objective to increase its temperature. The control of the inverter has been designed in such a way that it is easy to try waveforms different than the classical sine waves to see its effect on the temperature of the sample.

Although the research is one of the early stages, the results show that this technique could be a real option in the future.

I.- INTRODUCTION

Thermal therapies have been used along decades as a mean to help the recovery from several diseases, mainly as a complementary mean to the use of drugs and or mechanical manipulations depending on the specific application [1]. In particular, cancer is a quite well suited disease to be treated with heat since cancer cells are more sensitive to heat than healthy ones. In fact, temperature increases over 43º for several minutes can seriously damage those cells, which die by apoptotic mechanisms some hours after the treatment, while the rest of the cells survive [2]. Heating is also a well-suited therapy against cancer since tumors are quite un-receptive to therapeutic molecules for several reasons, and especially in hard to access places like the brain parenchyma [3]. However, either using ultrasounds or different kinds of electromagnetic sources, all conventional techniques suffer from the same drawbacks: not enough spatial resolution; precision in the localization of the volume where to deposit the thermal energy; and, the worst, the need for the applied radiation to cross healthy tissues to get to the desired area. These tissues may receive an even larger amount of energy than the targeted ones becoming unnecessary heated as well [4]. Although some efforts are in progress to improve conventional techniques like the case of Focused Ultrasounds, other new ones are being investigated to overcome those limiting performances. They use some intermediate agents previously deployed in place. These agents receive the energy, assuming that it travels throughout the living tissues without affecting them. They convert part of the energy into heat, thus heating their surroundings. This way, each problem is fitted at a different level: spatial resolution and localization is solved by correctly

deploying the agents, what is mainly a chemo-physiological problem, and the amount of energy and its application is mainly a matter of the energy source.

One of these new techniques is the so-called Magnetic Hyperthermia [5,6]. The energy comes from a radiofrequency source of some hundreds of kilohertz and consequently, nanoparticles of ferromagnetic materials (some tenths of nanometers) are used as intermediate agents. Radiofrequency also heats the living tissues due to their conductive character. However this drawback can be corrected by limiting the power of the source. This inconvenience is largely compensated by the fact that the corresponding wavelength is large enough to bring the energy no matter the place in the body. The particles become magnetized when the radiofrequency is present and start vibrating, either their whole body or their inner magnetic momentum, or both. Whatever the mechanism of interaction between particles and radiofrequency is, the mechanical energy is transformed into heat.

At this point one field of research is how to place the particles in place (and what kind of particles) in a safe and effective way, and other is how to excite those particles to maximize the heating. Of course, the goal is to reduce as much as possible the amount of delivered particles and energy, while keeping the therapeutic efficacy. Although both fields are tightly related and the whole approach could be seen as composed of many more faces, there is room to work with some independence in the excitation problem field. At this point, the state of the art is based on the use of sinusoidal waveforms for the radiofrequency emitter, since they are easily obtained at the moderately high power needed from the resonant circuits. Actually, it is not so much a matter of power, as of to heat the particles is rather small since the amount of particles is not so high. However, the ferromagnetic material when distributed as particles well under a micron diameter, to mention a common limit, becomes super-paramagnetic. Super-paramagnetic materials do not develop remanent magnetic fields and need higher magnetic saturation. The more the magnetization of the particles, the larger the amount of radiated energy converted into heat. Therefore, the issue of the amplitude is of great importance. The resonant circuits have been used as an instrument for this since they can provide radiofrequency power of high amplitude. The amount of power is not high but, in principle, it is not necessary for this purpose.

Few works have been carried on to explore other waveforms, although has been demonstrated for ferromagnetic particles, that a higher efficiency than conventional sinusoidal excitation can be achieved [7]. The mechanism converting the radiofrequency energy in heat is different in the case of ferromagnetic materials. However, since the size of the particles made of super-paramagnetic materials is smaller, they are very useful as intermediate agents in the living tissues for histological reasons.

The question about the use of other waveforms with super-paramagnetic particles is open. The interaction of these particles with the liquid environment where they are in suspension is really complex and still rather unknown. However, a previous work, still unpublished, points out to the

existence of a dependency of the losses in the particles on the amplitude of the magnetic field different from the theoretical one for low fields. At the same time, the stationary movement of the particles, achieved when using harmonic excitation, could tend to reduce the efficacy of the dissipation mechanisms.

To check all these issues in the search for more efficient ways to provide the radiofrequency energy for future magnetic hyperthermia based therapies, we have developed a new instrument that is presented in this work. Like in other cases [8-11], a power electronics circuit, helps a lot when it comes to developing a new research for medical purposes.

The main contribution of this instrument is that it allows testing with waveforms different than sine waves in an easy way. The instrument is composed by a power stage and control stages both explained in section II. The element that generates the magnetic field is an inductor which is analyzed in section III. In section IV, the set-up is described and, finally, the experimental results are shown in section V.

II.- POWER INVERTER

The circuit required to generate the alternating magnetic field is a full bridge inverter (Fig. 1). Nothing special is required since a simple phase shift control is enough to configure the maximum current, the current slope and the switching frequency. From the point of view of the power electronics design, the main challenge is to reduce the power losses when it operates in the MHz range.

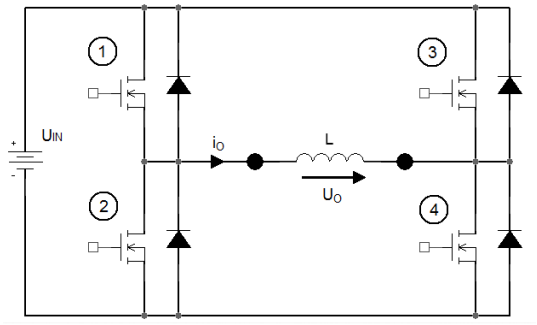

Fig. 1.- Power inverter

The main specifications of this configurable inverter are:

- Nominal Switching frequency: 800kHz although it should operate up to 2MHz
- Peak current: ±8A at 800kHz but up to 15A at lower frequencies
- Maximum current slew rate: 50A/µs. This forces to have a small inductor or a high input voltage. Since the inductor will be in the range of 10µH, the input voltage should be around 500V.

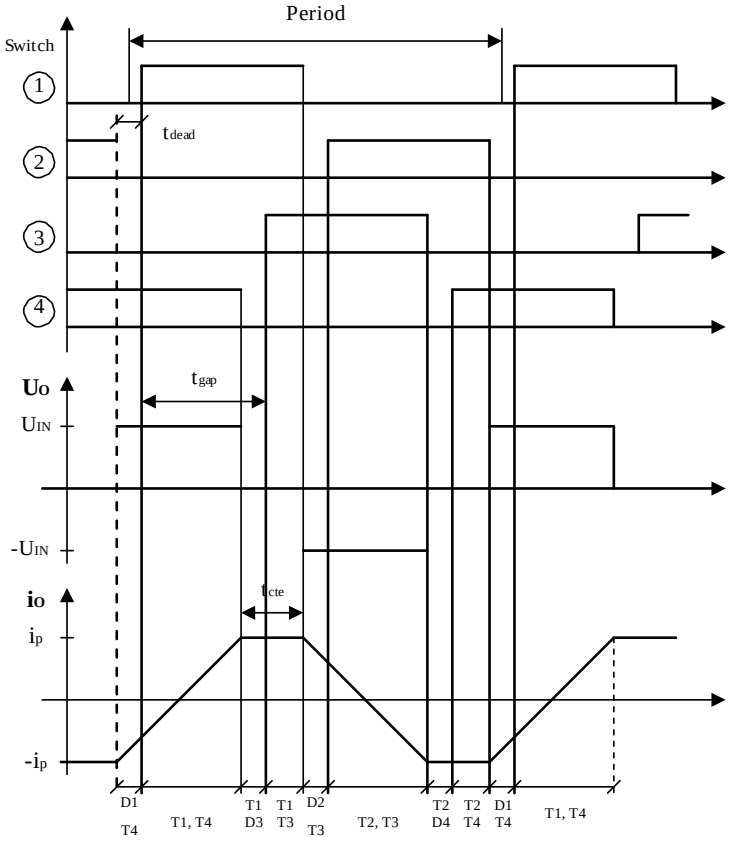

Fig. 2.- Gate signals, output voltage and output current

Playing with both the input voltage and the phase-shift angle, it is possible to vary the trapezoidal output current (Fig. 2) to triangular or "almost" square waveform. The maximum achievable current depends on both input voltage and switching frequency. Assuming that the current is triangular (t_{cte}=0 in Fig. 2) and the inductor is equal to 10µH, the maximum peak current is shown in Fig. 3. The converter will work in different operating points to perform experiments with the samples of nanoparticles. In case of using a trapezoidal current, the maximum current will be smaller since part of the period is used to keep the current constant (t_{cte}>0).

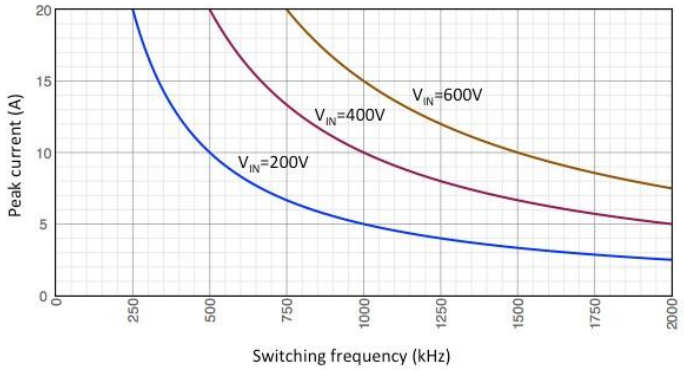

Fig. 3.- Maximum peak current as a function of the input voltage and the switching frequency

Optimization of the power stage in terms of power losses has been carried out obtaining a circuit that provides the desired current with relatively small losses. Table I shows the power losses analysis on the transistors. Considering the better performance in high frequency switching applications, the best design is obtained using SiC MOSFETs as predicted in [8]. Another advantage of the selected device is reflected in the fact that, if necessary, a higher slew rate could be achieved since the breakdown voltage is very high (1200V).

Device	Manufacturer	Material	Max. Vds (V)	Rdson (mΩ)	Losses (W)
IPA60R125CP	Infineon	Si	600	125	4,25
IPA60R160C6	Infineon	Si	600	160	4,75
STF25NM60ND	ST	Si	600	130	4,33
C2M0080120D	Cree	SiC	1200	98	2,88
CMF10120D	Cree	SiC	1200	200	5,42
TPH3006PS	Transphorm	GaN	600	180	4,83
PGA26A10	Panasonic	GaN	600	150	3,89

Table I.- Power losses on the power MOSFETs

It is important to realize that since the load is an inductor, it is very easy to achieve zero voltage switching (ZVS) at the turn-on of the four switches with an appropriate timing of the gate signals [11-16]. The dead time required to achieve ZVS is:

$$t_{dead} = \frac{L \cdot I_{max}}{V_{in}} \quad (1)$$

where C_{oss} is the output capacitance of the power switches. The time required to charge/discharge the parasitic capacitances depends on the inductor current and the input voltage. The selected device has a small output capacitance (80pF) being possible to obtain ZVS easily. For instance, with an inductor current equal to 8A and input voltage 400V, only 16ns are required to achieve ZVS, which is negligible compared with the switching period.

III.- Optimization of the Inductor

The purpose in this section is to design an inductor with air core that it is able to provide a high electric field in the center of it. The factors that have been considered for this optimization are: number of turns, wire diameter, radius of the inductor and separation of the turns. The optimization of the inductor has been carried out using a finite element analysis tool, namely Maxwell 2D. This tool has been used in [17] to extract a model of the magnetic component and in [18] to improve the connection of paralleled wires. In this case, the simulation is simpler since it is a winding with no core and with axisymmetric shape.

The starting point is an inductor that was available from the previous version of the instrument and this inductor was not designed according to high-frequency requirements. It should be considered that there are some physical constrains that limit the degrees of freedom in the design. In particular, the probe with the nanoparticles (explained in the experimental results sections) forces to have a minimum radius of 29 mm.

This inductor was made with 10 turns of 4mm diameter copper wire. It is 10 cm tall and there is a big separation between turns (around 1 cm but not homogeneous). With this inductor and with a peak current of 9A, the flux density in the center is around 0.6mT (this value has been obtained from the finite element analysis simulation and it is shown in Fig. 4a). It is obvious that this inductor has a very high leakage flux due to the separation of the turns and a further optimization is mandatory. The optimization process has been carried out in several steps:

a) Reduce the gaps between turns (design #2)

b) Reduce the radius of the inductor (design #3)

c) Increase the number of turns (design #4)

d) Replace single wire by twisted wires (design #5)

Table II shows the main data obtained from these simulations whereas the plots of the flux density for these four cases are shown in Fig. 4.

Test	Original	Design #2	Design #3	Design #4	Design #5
Number of turns	10	10	10	14	14
Number of wires x diameter (mm)	1 x 4	1 x 4	1 x 4	1 x 4	30 x 0.55

Radius of the inductor (mm)	35	35	29	29	29
B (mT) at center	0.93	1.35	1.56	1.86	1.95
Rac (mΩ) at 1MHz	60	264	200	339	614

Table II.- Results obtained from the simulation with the FEA tool

In design #2, the magnetic field is increased compared to the original design since there is less leakage; however proximity effect increases the AC resistance. The design #3 shows a good improvement since the reduction of the radius increases the flux at the center and reduces the length of the inductor and thus the resistance. The design #4 has more turns and therefore the field is higher; in addition resistance is increased. Finally, last design shows a slightly higher field but proximity effect is also very high, increasing very much the AC resistance. All these data have been obtained introducing a 800Hz sine wave with 9A peak current.

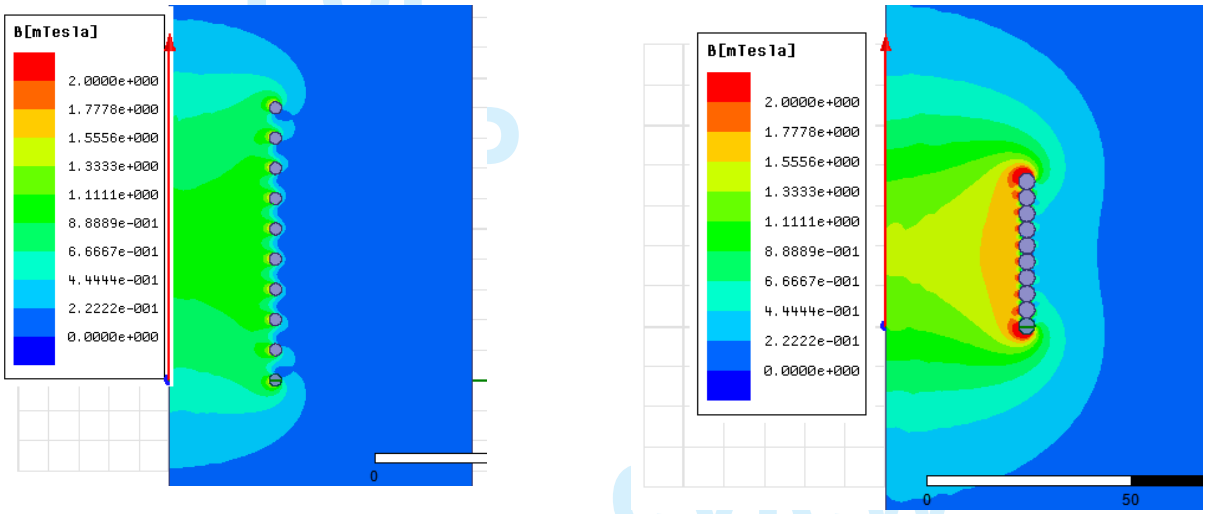

(a) (b)

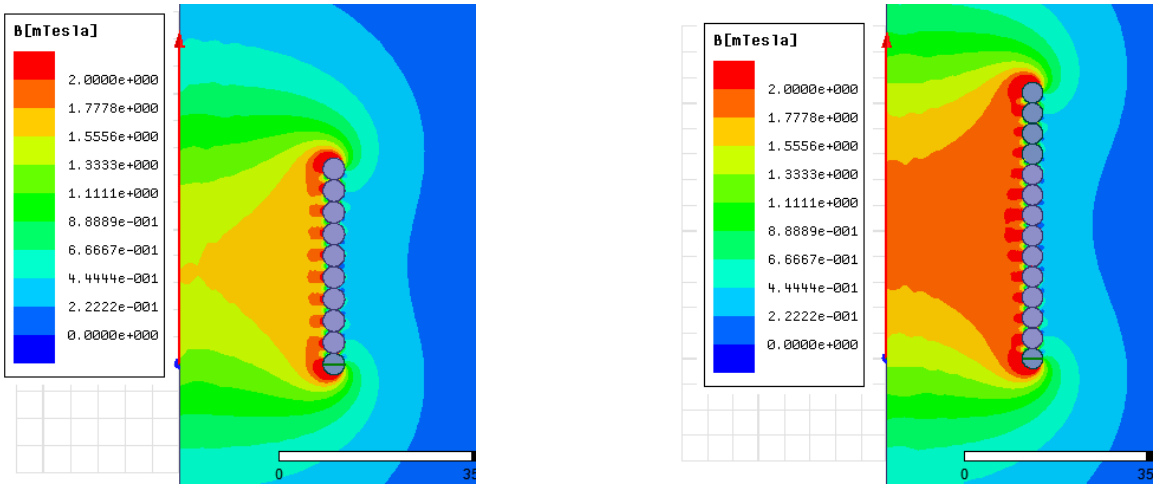

(c) (d)

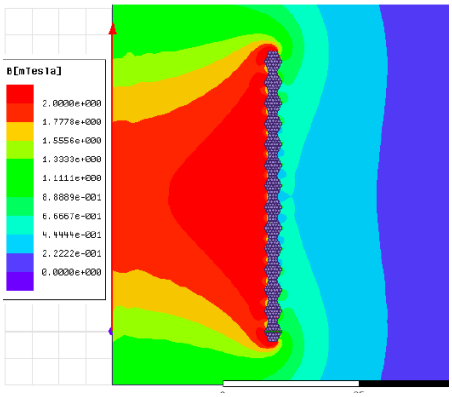

(e)

Fig. 4.- Flux density simulation obtained from the FEA tool: original inductor(a), design #2 (b), design #3 (c), design #4 (d) and design #5 (e)

With this last inductor (Fig. 4e), the flux density in the sample is more than three-times higher (1.95mT) compared to the original and, for this reason, this design has been selected.

Another thing that can be extracted from the simulations is that, the power losses in the inductor increase with every new design. In the last one, the power losses may become very important at high frequency. However, it should be noted that the simulation of the design #5, is very sensitive to small changes in distance among wires. The simulation of this design has been repeated including 0.1mm among wires decreasing the ac resistance to 445mΩ. Fig. 5 shows picture of the preliminary inductor and the design #5.

Fig. 5a.- Picture of the preliminary inductor

Fig. 5b.- Picture of the implemented inductor (design #5)

IV.- SET-UP DESCRIPTION

Fig. 6 shows a diagram of the instrument and the experimental set-up. It has three different parts: power electronics circuit with inductor, probe with nanoparticles and temperature sensing and recording.

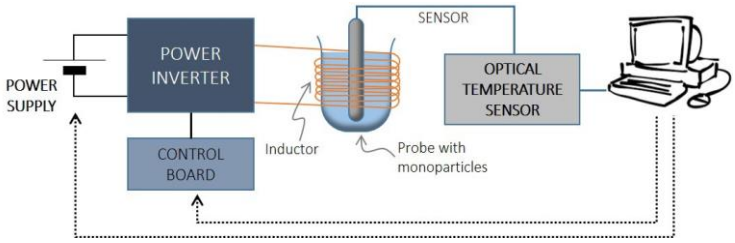

Fig. 6.- Experimental set-up

The control board generates the pulses for the power transistors of the inverter. It is based on an FPGA previously configured such that produces different types of pulses. The board contains a simple interface for the user (micro-switches, SMD buttons and LED indicators) that allows an easy open-loop control of the converter. The inverter is shown in Fig. 7a and the control board in Fig. 7b. The inverter is loaded with an inductor (Fig. 5b). The measurement of this inductor shows an inductance of 10.7µH and the ac resistance of 905mΩ at 1MHz.

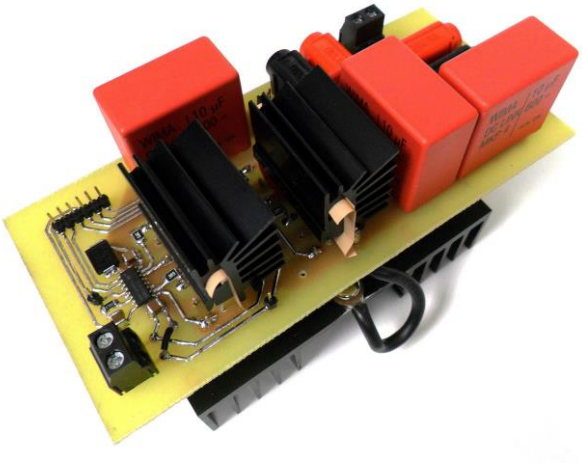

Fig. 7a.- Power inverter designed for these experiments

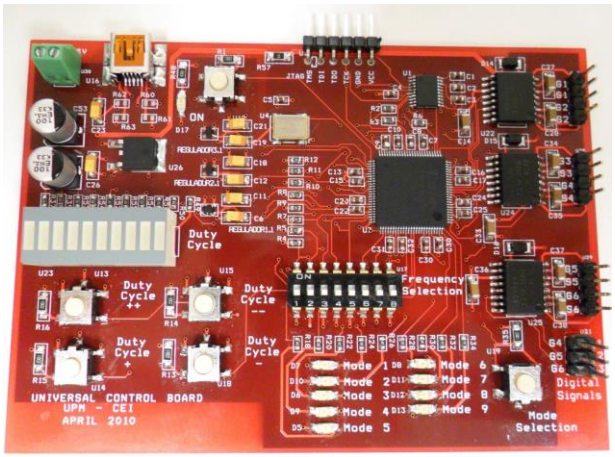

Fig. 7b.- Control board of the inverter

In this stage of the research, it is possible to operate in an open loop; in a future scenario, it would be necessary to close the loop and be more accurate to obtain a better relation between electric field (i.e. current) and heating. An interface between the PC and the control board is being build now for this purpose (dotted line in Fig. 6).

The parameters that can be controlled with this board are switching frequency, phase delay and dead-time between transistors. With these parameters and the input voltage of the converter, it is possible to generate different current waveforms on the inductors like the ones in Fig. 8.

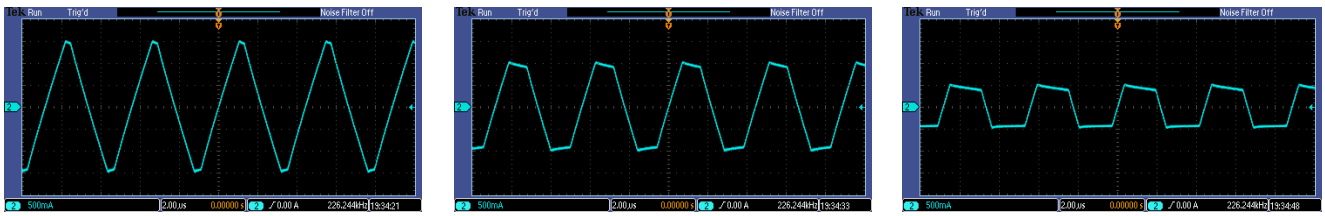

(a) (b) (c)

Fig. 8.- Capture of the different current shapes: triangular (a), trapezoidal (b) and "almost" square (c)

The main objective is to design an instrument that generates a configurable magnetic field and to measure its effect on the temperature of the sample with a particular concentration of nanoparticles. It is very important to assure a very good thermal isolation between the probe and the inductor. For this purpose, the nanoparticles will be in the center of a structure with a vacuum chamber surrounded by a constant temperature water flux. With it, the effects of the power losses on the copper wires of the inductor do not have an impact on the temperature of the nanoparticles. Fig. 9 shows a description of this probe.

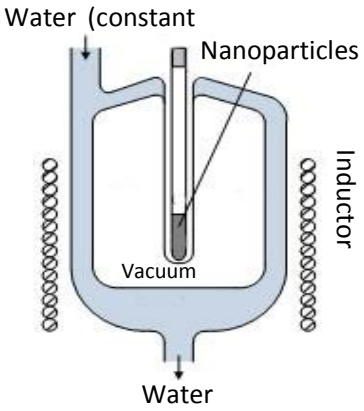

Fig. 9.- Description of the probe

Super-paramagnetic iron oxide nanoparticles (SPION) were synthesized following the method described by Lin [18]. The resulting solid was dried to get a Fe_3O_4 powder. Synthesized SPION were characterized by transmission electron microscopy and powder X-ray diffraction. Representative images of the solid show well-defined nanoparticles with an average diameter of 14 nm. Powder X-ray diffraction pattern showed the typical reflections of Fe_3O_4 in the range $25° < 2\theta < 65°$ (Fig. 10). To perform the hyperthermia experiments, nanoparticles were suspended in an aqueous solution at a concentration of 5mg/ml.

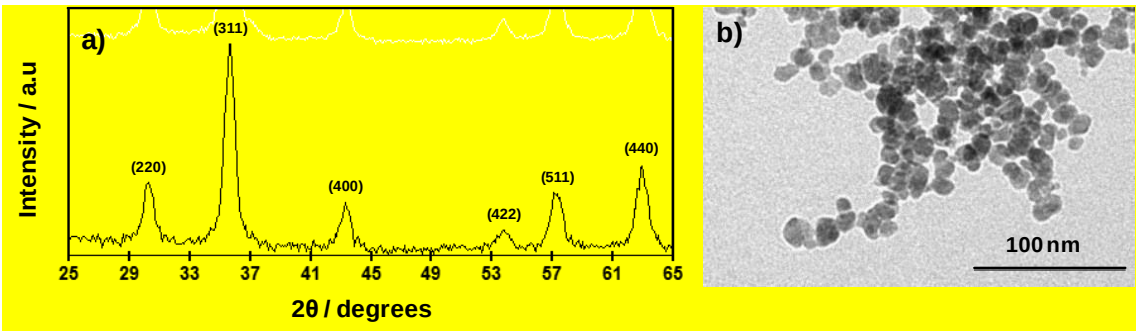

Fig. 10. a) Powder X-ray diffraction pattern and b) Transmission Electron microscopy representative image of synthesized SPION.

V.- EXPERIMENTAL RESULTS

Several experiments have been carried out to measure the effect of the magnetic field in the sample. Table III summarizes these tests. The experiment #1 is done without nanoparticles, just to confirm that the heat generated in the inductor does not produce any temperature increment in the sample. In the rest of experiments, the sample was made 14nm Fe_3O_4 nanoparticles.

Test	Frequency (kHz)	Shape of field	Voltage (V)	Peak Current (A)	Time (min)	Δ Temperature (ºC)
#1	800	Trapezoidal	380	9	40	0 (no nanoparticles)
#2	303	Trapezoidal	195	12	24	1.5
#3	303	Trapezoidal	235	14	10	1.5
#4	510	Trapezoidal	286	10.5	34	1.6
#5	800	Trapezoidal	380	9	35	2.1
#6	800	Trapezoidal	470	11	25	2.1
#7	800	Square	490	6	28	1.3
#8	800	Triangular	205	6	20	2.7
#9	800	Triangular	410	12	13	2.7
#10	1315	Square	500	6	25	1.7
#11	1315	Triangular	370	6	20	2.2
#12	1315	Triangular	500	8.2	10	2.2

Table III.- Experiments carried out using the inverter and the inductor. The temperature is measured in a thermally isolated probe with nanoparticles located in the center of the inductor

Fig. 11 shows two experimental data obtained from the tests. The obtained temperature increments could be enough to kill bad cells by inducing localized fever in the patient.

The conclusion that can be extracted is that with this instrument, significant increments of temperature are achieved for non-sinusoidal waveforms, being the first time that this is published. In most of the cases, these tests are useful to see dependences but not to extract quantitative values. The temperature increments seem to be very correlated with the amplitude of the current; the same can be said about the frequency of the magnetic field, but not in all cases. At this moment, it is not possible to extract clear conclusions about the influence of the shape of the field in the temperature. However, the results seem very promising and now that the equipment is available, many more experiments will be carried out. The next steps in this research are: identify the best magnetic field (shape and frequency) and apply it to a sample of nanoparticles in a concentration compatible with the body cells; to check the effect of the temperature in the cells; and to obtain percentages of success in killing bad cells.

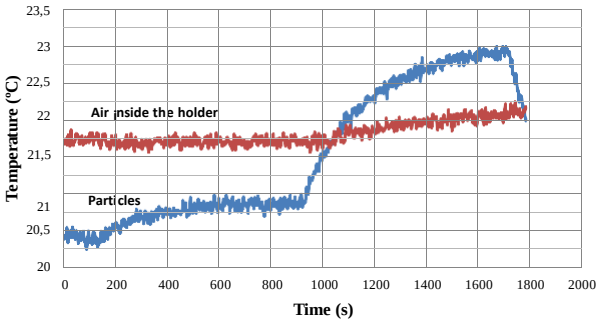

Fig. 11a.- Experimental temperature increment in test #5

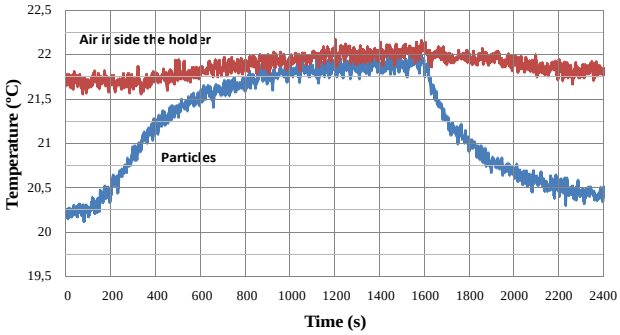

Fig. 11b.- Experimental temperature increment in test #10

V .- CONCLUSIONS

The purpose of this work is to design a configurable power inverter to induce heating in a sample with nanoparticles, as a first step to improve the magnetic hyperthermia technique. The inverter allows tests with different parameters of the magnetic field such as frequency, intensity and shape. The combination of these three parameters may show the best way to continue the research with this technique. By the moment, temperature increments beyond 2.5ºC have been achieved, being a very promising result since this is the first time that a non-sinusoidal waveform is used for this purpose. From the point of view of power electronics, the success is achieved thanks to an optimized design of the full-bridge inverter (ZVS and low losses), and especially to the inductor, that maximizes the field in the position where the sample with nanoparticles is located.

IV.- REFERENCES

[1] W. C. Dewey, L. E. Hopwood, S. A. Sapareto, and L. E. Gerweck, "Cellular responses to combinations of hyperthermia and radiation," Radiology, vol. 123, no. 2, pp. 463–474, 1977.

[2] Wang, X.; Yang, L.; Chen, Z.; Shin, D.M. "Application of Nanotechnology in Cancer Therapy and Imaging." CA Cancer J Clin 2008, 58, 97–110

[3] Brandes A A, Tosoni A, Franceschi E, Reni M, Gatta G and Vecht C 2008, "Glioblastoma in adults" Crit Rev Oncol Hematol 67 139-52

[4] A.B. Salunkhe, V.M. Khot and S.H. Pawar, "Magnetic Hyperthermia with Magnetic Nanoparticles: A Status Review", Current Topics in Medicinal Chemistry, 2014, 14, 000

[5] G Vallejo-Fernandez, O Whear, A G Roca, S Hussain, J Timmis, V Patel and K O'Grady, "Mechanisms of hyperthermia in magnetic nanoparticles", J. Phys. D: Appl. Phys. 46 (2013) 312.001 (6pp)

[6] Hiroaki Mamiya, "Recent Advances in Understanding Magnetic Nanoparticles in AC Magnetic Fields and Optimal Design for Targeted Hyperthermia", Journal of Nanomaterials, Volume 2013, Article ID 752973, 17 pages

[7] Eiji Kita, Tatsuya Oda, Takeru Kayano, Suguru Sato, Makoto Minagawa, Hideto Yanagihara, Mikio Kishimoto, Chiharu Mitsumata, Shinji Hashimoto, Keiichi Yamada and Nobuhiro Ohkohchi, "Ferromagnetic nanoparticles for magnetic hyperthermia and thermoablation therapy", J. Phys. D: Appl. Phys. 43 (2010) 474011 .

[8] Kassakian, J.G.; Jahns, T.M., "Evolving and Emerging Applications of Power Electronics in Systems," Emerging and Selected Topics in Power Electronics, IEEE Journal of , vol.1, no.2, pp.47,58, June 2013

[9] Bondade, R.; Yikai Wang; Dongsheng Ma, "Design of Integrated Bipolar Symmetric Output DC–DC Power Converter for Digital Pulse Generators in Ultrasound Medical Imaging Systems,"Power Electronics, IEEE Transactions on , vol.29, no.4, pp.1821,1829, April 2014

[10] Valente, V.; Eder, C.; Donaldson, N.; Demosthenous, A., "A High-Power CMOS Class-D Amplifier for Inductive-Link Medical Transmitters," Power Electronics, IEEE Transactions on , vol.30, no.8, pp.4477,4488, Aug. 2015

[11] J.A. Sabate,V. Vlatkovic, R.B. Ridley, F.C. Lee, B.H. Cho, "Design considerations for high-voltage high-power full-bridge zero-voltage-switched PWM converter," Applied Power Electronics Conference and Exposition, 1990. APEC '90, Conference Proceedings 1990., Fifth Annual , vol., no., pp.275-284, 11-16 March 1990.

[12] G. Hua, F.C. Lee, "Soft-switching techniques in PWM converters", IEEE Transactions on Industrial Electronics, vol.42, no.6, pp.595-603, Dec 1995.

[13] Ki-Bum Park; Chong-Eun Kim; Gun-Woo Moon; Myung-Joong Youn; , "Voltage Oscillation Reduction Technique for Phase-Shift Full-Bridge Converter," Industrial Electronics, IEEE Transactions on , vol.54, no.5, pp.2779-2790, Oct. 2007.

[14] R. Redl, N.O. Sokal, L. Balogh, "A novel soft-switching full-bridge DC/DC converter: Analysis, design considerations, and experimental results at 1.5 kW, 100 kHz," Power Electronics Specialists Conference, 1990. PESC '90 Record., 21st Annual IEEE , vol., no., pp.162-172, 0-0 1990.

[15] R. Watson, F.C.,"A soft-switched, full-bridge boost converter employing an active-clamp circuit," Power Electronics Specialists Conference, 1996. PESC '96 Record., 27th Annual IEEE ,vol.2, no., pp.1948,1954 vol.2, 23-27 Jun 1996.

[16] Prasanna, U.R.; Rathore, A.K., "Extended Range ZVS Active-Clamped, Current-Fed Full-Bridge Isolated DC/DC Converter for Fuel Cell Applications: Analysis, Design, and Experimental Results," Industrial Electronics, IEEE Transactions on , vol.60, no.7, pp.2661,2672, July 2013.

[17] R. Prieto, R. asensi, J.A. Cobos, J. Uceda, "A full procedure to model integrated magnetics based on FEA", IEEE Applied Power Electronics Conference APEC 2004, Vol. 2, Pages: 952 – 957

[18] R. Prieto, R. asensi, J.A. Cobos, J. Uceda, "Selection of the appropriate winding setup in planar inductors with parallel windings", IEEE Energy Conversion Congress and Exposition ECCE 2010

[19] S. Giri, B.G. Trewyn, M.P. Stellmaker, V.S.-Y. Lin, "Stimuli-Responsive Controlled-Release Delivery System Based on Mesoporous Silica Nanorods Capped with Magnetic Nanoparticles†", Angewandte Chemie International Edition, Volume 44, Issue 32, pages 5038–5044, August 12, 2005